Supplementary material: Analysis of the radial distribution function

The effect of the wall can be characterised by the radial distribution function $g_{pp}(r_k)$, which is a measure of the probability increase of finding a second particle at a distance $r_k \pm \Delta r/2$ from another particle. The computation of the radial distribution function should take into account the spatial inhomogeneity and temporal unstationarity of the particle density in the fluidised bed. The mean radial distribution function in a post-processing cell C_n is computed as

$$g_{pp}(r_k) = \frac{\langle n_{pp}(r_k)\rangle^n}{\langle n_p\rangle^n \langle n_{\text{Shell}}(r_k)\rangle^n}, \tag{0.1}$$

where $n_{pp}^{n,\ell}(r_k)$ is the number of particle duplets per unit volume squared at time t_ℓ that are separated by a distance $r_k \pm \Delta r/2$ and with a least one of the particles in cell C_n,

$$n_{pp}^{n,\ell}(r_k) = \frac{1}{4\pi r_k^2 \Delta r V_n} \sum_{i=1}^{N_p} \sum_{j=1}^{N_p} \left[\boldsymbol{x}_p^{i,\ell} \in C_n\right] \left[r_k - \tfrac{\Delta r}{2} < \|\boldsymbol{x}_p^{j,\ell} - \boldsymbol{x}_p^{i,\ell}\| \leqslant r_k + \tfrac{\Delta r}{2}\right], \tag{0.2}$$

with $n_p^{n,\ell} = (1/V_n)\sum_{i=1}^{N_p}\left[\boldsymbol{x}_p^{i,\ell} \in C_n\right]$ the number of particle centres per unit volume in cell C_n and $n_{\text{Shell}}^{n,\ell}(r_k)$ the expected number of particle centres per unit volume in the union of the spherical shells of radius $r_k \pm \Delta r/2$ of the particles contained within cell C_n. The particle density $n_{\text{Shell}}^{n,\ell}(r_k)$ is estimated by randomly sampling points within C_n,

$$n_{\text{Shell}}^{n,\ell}(r_k) = \frac{1}{4\pi r_k^2 \Delta r N_{\text{spl}}} \sum_{i=1}^{N_{\text{spl}}} \sum_{j=1}^{N_p} \left[r_k - \tfrac{\Delta r}{2} < \|\boldsymbol{x}_p^{j,\ell} - \boldsymbol{x}_{\text{spl}}^{i,\ell}\| \leqslant r_k + \tfrac{\Delta r}{2}\right], \tag{0.3}$$

where N_{spl} is the number of sampled points and $\boldsymbol{x}_{\text{spl}}^{i,\ell}$ the position vector of the i-th sampled point. The peaks in the radial distribution function (figure 1) are associated with the presence of assemblies with an orderly arrangement (Wensrich 2012). In particular, the peaks r_{ij} of a two-dimensional hexagonal arrangement are of the form

$$\frac{r_{ij}}{d_p} = \begin{cases} \frac{1}{2}\sqrt{4i^2 + 3j^2} & \text{if } j \text{ even} \\ \frac{1}{2}\sqrt{4\left(i + \frac{1}{2}\right)^2 + 3j^2} & \text{if } j \text{ odd} \end{cases} \tag{0.4}$$

with i and j two integers. Close to the wall, the CFD-DEM radial distribution function in figure 1(a, c, e) clearly exhibits all the peaks of a two-dimensional hexagonal arrangement. This is consistent with the presence of particle assemblies with a two-dimensional hexagonal arrangement near the wall. In addition, the peaks of the three-dimensional face-centred cubic (FCC) arrangement can be identified. Note that while the peaks of the CFD-DEM radial distribution function may also be found in a three-dimensional hexagonal close packing (HCP) arrangement, we would expect the CFD-DEM radial distribution function to exhibit additional peaks in the presence of assemblies with such an arrangement. The peaks of the CFD-DEM radial distribution function are sharper and more clearly defined in the case F3 (figure 1(c)) than in the case F3-Frictionless (figure 1(e)). The friction at the wall favours the orderly arrangement of the particles at the wall since it decreases the particle slip velocity, and make the particles in contact with the wall more resistant to disturbances. Note that the friction associated with particle-particle contacts, which is neglected in our simulations, may also influence the orderly arrangement of the particles (Wensrich 2012). The peaks are furthermore sharper and more clearly defined in the case F4 (figure 1(a)) than in the case F3 (figure 1(c)). This can be attributed to the larger solid volume fraction and lower

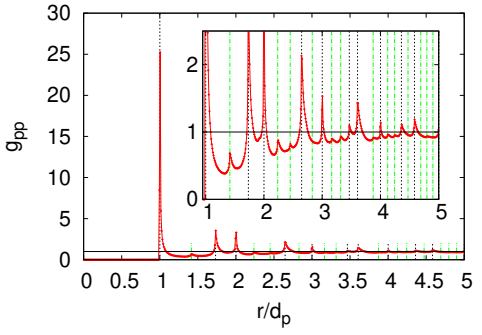

(a) F4, $0 < \check{r}_w < 1$

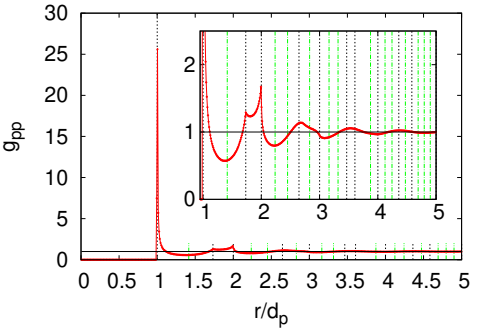

(b) F4, $10 < \check{r}_w < 11$

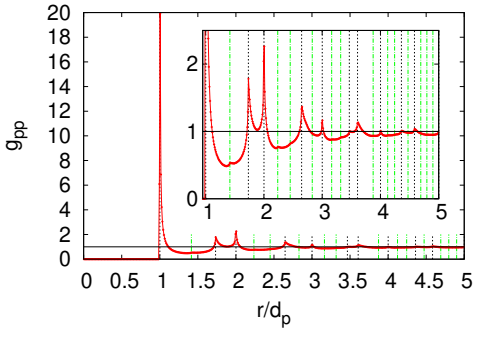

(c) F3, $0 < \check{r}_w < 1$

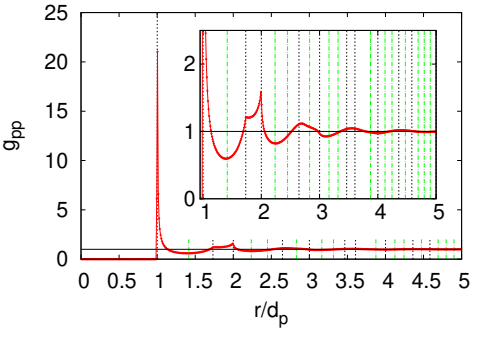

(d) F3, $10 < \check{r}_w < 11$

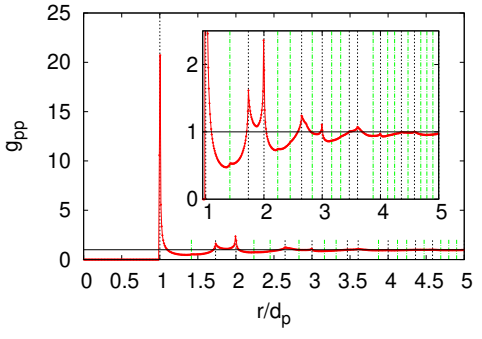

(e) F3-Frictionless, $0 < \check{r}_w < 1$

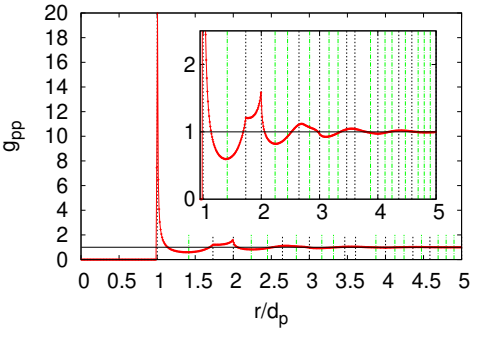

(f) F3-Frictionless, $10 < \check{r}_w < 11$

Figure 1: Radial distribution function at the height $z/R_c = 3.45$ in the case F4, F3 and F3-Frictionless (a, c, e) close to the wall, namely for particles whose centre is located within $\check{r}_w = (R_c - r_p)/d_p = 1$ particle diameters of the wall, and (b, d, f) far from the wall, namely for particles whose centre is $\check{r}_w = 10$ to 11 particles diameters away from the wall. The dashed vertical lines are the peaks of a two-dimensional hexagonal arrangement, namely 1, $\sqrt{3}$, 2, $\sqrt{7}$, 3, $\sqrt{12}$, $\sqrt{13}$, 4, $\sqrt{19}$ and $\sqrt{21}$. The dot-dashed vertical lines are the peaks $\sqrt{2}$, $\sqrt{5}$, $\sqrt{6}$, $\sqrt{8}$, $\sqrt{10}$, $\sqrt{11}$, $\sqrt{15}$, $\sqrt{17}$, $\sqrt{18}$, $\sqrt{20}$, $\sqrt{22}$, $\sqrt{23}$ and $\sqrt{24}$, which are not found in a two-dimensional hexagonal arrangement but are found in a three-dimensional FCC arrangement.

particle velocity of that case. Far from the wall, the CFD-DEM radial distribution function in figure 1(b, d, f) exhibits the split second peak first reported by Finney (1970*a*,*b*). However, no clearly defined peak is observed at greater separation distances for any of the CFD-DEM simulations. This is consistent with the scarcity of orderly arrangements far from the wall, compared to the near-wall region.

REFERENCES

Finney, J. L. 1970*a* Random packings and the structure of simple liquids. I. The geometry of random close packing. *Proceedings of the Royal Society of London. A. Mathematical and Physical Sciences* **319** (1539), 479–493.

Finney, J. L. 1970*b* Random packings and the structure of simple liquids. II. The molecular geometry of simple liquids. *Proceedings of the Royal Society of London. A. Mathematical and Physical Sciences* **319** (1539), 495–507.

Wensrich, C. M. 2012 Boundary structure in dense random packing of monosize spherical particles. *Powder Technology* **219**, 118–127.